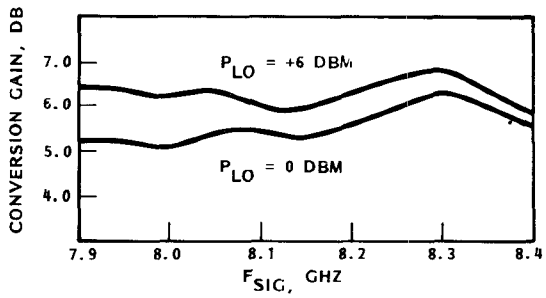

Fig. 7. Gain of Mixer no. 2 (AT8060 FET). The LO level for optimum noise figure is 0 dBm; optimum third-order intermodulation is +6 dBm. $V_{ds} = 3.0$ V, $V_{gs} = -1.0$ V.

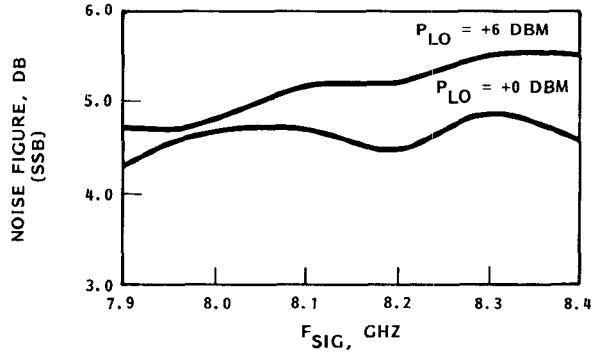

Fig. 8. Noise figure of Mixer no. 2 at the LO level for optimum noise (0 dBm) and optimum intermodulation (+6 dBm). DC bias for both cases is $V_{ds} = 3.0$ V, $V_{gs} = -1.0$ V.

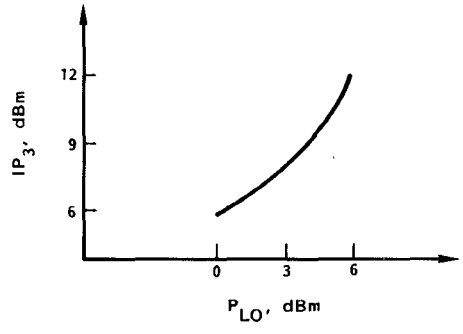

Fig. 9. Third-order intermodulation intercept point of mixer no. 2, as a function of LO level. DC bias is the same as that used for noise figure data.

and −1.0 V, respectively. As with the first mixer, the gate is biased close to pinchoff.

It is worthwhile to compare these results to the performance of diode mixers. Commercially available balanced diode mixers used most often in the microwave range exhibit conversion losses of 5–9 dB, third-order intercept points (output) of 0–13 dBm, and have LO power requirements of 8–18 dBm. It is possible in some cases to achieve mixer noise figures as low as 3.5 dB by narrow-band design and image enhancement, and receiver noise figures around 5 dB. Such mixers require considerable effort to design and optimize, and will almost certainly be single-ended structures with relatively poor intermodulation performance. Multidiode balanced mixers offer better intermodulation performance, approaching that of FET mixers, at the expense of high LO power requirements. However, most balanced structures cannot be tuned and optimized as effectively as single diode mixers, so their noise performance is usually worse. The FET mixer offers lower noise and equal or better linearity with less LO power. It can be incorporated into balanced structures for even lower intermodulation without sacrificing noise performance or creating a terrifying design problem.

V. Conclusions

A very general theory of active mixers has been presented, with application to GaAs FET mixers. The theory has been validated experimentally.

Acknowledgment

The author wishes to thank Dr. N. Alexopoulos of UCLA, Los Angeles, CA, Dr. P. Greiling and Dr. D. Matthews of Hughes Aircraft Co., Torrence, CA, and Dr. J. M. Andres of TRW, Redondo Beach, CA, for helpful discussions, and J. Abell of TRW for assistance with the fabrication of the mixers.

References

[1] R. A. Pucel, D. Masse, and R. Bera, "Performance of GaAs MESFET mixers at X-band," *IEEE Trans. Microwave Theory Tech.*, vol. MTT-24, no. 6, pp. 351–360, June 1976.

[2] P. L. Ntake, "A computer-aided design of low-noise parametric down-converters and GaAs FET mixers for low-cost satellite microwave receivers," Ph.D. dissertation, Carleton Univer., Ottawa, Ont., Canada, 1977.

[3] P. Harrop, "GaAs FET mixers: Theory and applications," *Acta Electronica* (France), vol. 23, no. 4, pp. 291–297, 1980.

[4] O. Kurita and K. Morita "Microwave MESFET mixer," *IEEE Trans. Microwave Theory Tech.*, vol. MTT-24, pp. 361–266, June 1976.

[5] G. Begemann and A. Jacob, "Conversion gain of MESFET drain mixers," *Electron. Lett.*, vol. 15, no. 18, pp. 567–568, Aug. 30, 1979.

[6] G. Begemann and A. Hecht, "The conversion gain and stability of MESFET gate mixers," in *Proc. 9th European Microwave Conf.* (Brighton, England), Sept, 17–20, 1979, pp. 316–320.

[7] A. R. Kerr, "A technique for determining the local oscillator waveforms in a microwave mixer," *IEEE Trans. Microwave Theory Tech.*, vol. MTT-23, no. 10, pp. 828–831, Oct. 1975.

[8] A. R. Kerr, "Corrections to 'A technique for determining the local oscillator waveforms in a microwave mixer,'" private communication.

[9] S. Egami, "Nonlinear, linear analysis and computer-aided design of resistive mixers," *IEEE Trans. Microwave Theory Tech.*, vol. MTT-22, pp. 270–275, Mar. 1974.

[10] R. Pucel, H. A. Haus, and H. Statz, "Signal and noise properties of GaAs microwave field effect transistors," in *Advances in Electronics and Electron Physics*, L. Martin, Ed., vol. 38. New York: Academic Press, 1975, pp. 195–265.

Microwave Hyperthermic Distributions in a Layered Living Body with Nonlinear Thermoregulatory Properties

S. CAORSI

***Abstract*—In this paper, the microwave heating of biological systems with nonlinear thermoregulatory properties is considered. Temperature distributions are calculated in a layered biological model exposed to uniform plane waves. The external surfaces of such a model are cooled and its thermoregulatory properties are assumed to be nonlinear functions of the local temperature. The calculation of the space-time evolution of the temperature is performed using a numerical program that has been developed by applying the finite-difference method. In this numerical program, the nonlinear thermoregulatory functions are given either by a segment-linearization process or by an arbitrary analytical form or by a transformation of an input sample set. The mean power density of the incident electromagnetic wave and the coolant temperature are also taken time-dependent.**

Manuscript received November 22, 1983; revised April 23, 1984.

The author is with the Biophysical and Electronic Engineering Department, University of Genoa, Via all'Opera Pia, lla, 16145, Genova, Italy.

I. Introduction

As is well known, microwave hyperthermia in oncological therapy is based on the heating of cancerous tissues to keep them in the range of 41 to 45° C for a given period of time [1], [2].

During electromagnetic heating, the temperature distribution is not only dependent on the distribution of electromagnetic absorption, but also on the mechanism of heat generation and transfer, as well as on the initial and boundary conditions. Consequently, it is necessary to simulate mathematically, as accurately as possible, both the physical characteristics of the living body and the complex thermal processes taking place inside it.

The available theoretical contributions to the resolution of the above problem are based on simplified geometries of biological tissues and on the mathematical models that have been developed starting from the well-known equation of transient heat conduction [3].

Such models are characterized by internal heat generation and dissipation, which are generally considered as independent or linear functions of the local temperature [4]–[6]. The linear theoretical model was improved by assuming the mean power density of the incident plane wave and the coolant temperature to be time-dependent [7], [8].

Nevertheless, the linear approach seems to be insufficient to describe the complex thermal phenomena that characterize a living body [9], [10].

In this paper, to obtain the best possible approximation of the actual behavior of a biological system, we develop, in accordance with previous results [11]–[13], a mathematical model of heat conduction where the thermal processes related to metabolism and the blood flow are assumed to be nonlinear functions of the local temperature.

The biological system is represented by a set of plane layers with physical characteristics (e.g., complex dielectric permittivity, density, specific heat, etc.) that can be deduced from bibliographic references [2], [14], [15].

Such a biological system is irradiated by a plane wave, while the mean power density of the incident field and the coolant temperature are assumed to be time-dependent functions.

The calculation of the temporal evolution of the temperature distribution can be performed by a numerical program that we developed in accord with the finite-difference method.

II. Mathematical Model

We assume that a biological system can be simulated by a series of homogeneous plane layers, and that each layer is characterized by constant values of its complex dielectric permittivity, specific heat, and density. Moreover, the thermoregulatory properties of the living body are represented, as a first approximation, by the control of the metabolic heat production and by the control of the heat loss through the exchange with the cardiovascular system (i.e., variations in the blood flow) and with the environment surrounding the external surface of the body.

The biological system is exposed to uniform plane waves that normally impinge on its external surface; a coolant contacts its outer surface where the electromagnetic field is incident.

Under these conditions, the heat-conduction equation for each layer can be written as follows:

$$c_n g_n \frac{\partial}{\partial t} v_n(x,t) = \frac{\partial}{\partial x}\left(k_n \frac{\partial}{\partial x} v_n(x,t)\right) + Q_n^{tr}(v(x,t)) + Q_n^{em} \tag{1}$$

where

- $v_n(x,t)$ represents the time-space evolution of the temperature in the nth layer,
- c_n, g_n, k_n are the specific heat, density, and thermal conductivity, respectively,
- Q_n^{tr} represents the combined effect of the metabolic heat production and of the heat loss through the blood flow,
- Q_n^{em} represents heat production due to absorption of electromagnetic energy.

Under the assumption of plane waves normally impinging on the layered system, the heat production Q_n^{em} in each layer can be written as follows:

$$Q_n^{em}(x) = P_0 W_n(x)/J \tag{2}$$

$$W_n(x) = \tfrac{1}{2}\sigma_n |E_n(x)|^2 \tag{3}$$

where $E_n(x)$ is the electric-field distribution in the nth layer, P_0 is the mean power density of the incident plane wave, σ_n is the electric conductivity of the nth layer, and J is the mechanical equivalent of heat.

The electric-field distribution in each layer can easily be obtained by use of a transmission-line analogy. Then, in the nth layer

$$E_n(x)/E_0 = T_n\left(e^{-j\gamma_n(x-x_n)} + \rho_n e^{+j\gamma_n(x-x_n)}\right) \tag{4}$$

where E_0 is the amplitude of the incident field, γ_n is the complex propagation constant, $\gamma_n = \omega\sqrt{\mu_0 \epsilon_n}$, ϵ_n is the complex dielectric permittivity, x_n is the coordinate of the interface between the nth layer and the $(n+1)$ one, $x_n = \sum_{i=1}^{n} l_i$, l_i is the layer length, ρ_n is the reflection coefficient at the x_n plane

$$T_n = \frac{\prod_{i=1}^{n} t_i}{\exp\left(j \sum_{i=1}^{n} \gamma_i l_i\right)} \tag{5}$$

and

$$t_i = \frac{1+\rho_{i-1}}{1+\rho_i \exp(-2j\gamma_i l_i)}. \tag{6}$$

The reflection coefficient ρ_n is obtained by applying successively the impedance transformation along all the layers included between the nth layer and the last boundary plane $(n+1, n+2, \cdots, N)$. The reflection coefficient of the incident wave at $x = 0$ (i.e., ρ_0) is obtained in the same way, that is, by extending the transformation process to the first layer.

The system's nonlinearity is represented by the thermoregulatory effects Q_n^{tr} which are assumed to be nonlinear functions of the local temperature and are different in each layer, to better approximate the actual behaviors of the various biological tissues (fat, bone, muscle, liver, etc.).

In general, we can write

$$Q_n^{tr}(v) = A_n^*(v) v(x,t) + B_n^*(v). \tag{7}$$

This relation includes both the metabolic effect Q_n^m and the blood-flow effect Q_n^{bf} that is

$$Q_n^{tr} = Q_n^m + Q_n^{bf}. \tag{8}$$

If coefficients A_n^* and B_n^* are constant quantities, the behavior of the nth layer of the biological system is linear. In this case, we can consider, for example, a constant metabolic heat production and a linear heat exchange with the blood flow [5], [7], [11]

$$Q_n^{bf} = -B_n(v(x,t) - vb_n) \tag{9}$$

where B_n is the product of the flow and heat capacity of the blood, and vb_n is the temperature of the arterial blood entering the tissue.

To complete the problem statement, it is necessary to specify the boundary conditions at the interface between the various layers, as well as the conditions on the external surfaces. In the first case, the heat flow and the temperature must be continuous

$$k_n \frac{\partial}{\partial x} v_n(x,t)\Big|_{x_i} = k_{n+1} \frac{\partial}{\partial x} v_{n+1}(x,t)\Big|_{x_i} \tag{10}$$

$$v_n(x_i,t) = v_{n+1}(x_i,t) \tag{11}$$

$$x_i \in I_{n,n+1}$$

where $I_{n,n+1}$ represents the interface between the nth layer and the $n+1$ one. In the second case, we use the typical Cauchy condition [16]

$$\frac{\partial}{\partial n} v_n(x,t)|_{x_s} = -\beta_s(v_n(x_s,t) - ve_s(t)) \tag{12}$$

where x_s represents the coordinate of the boundary plane surfaces ($x_s = 0, n = 1$, and $x_s = 1, n = N$; 1: total length of the layered system); $\partial/\partial n$ stands for the outgoing normal derivative; and ve_s can be both the temperature of the environment surrounding the boundary surface and the temperature of the cooling medium.

Finally, we assume that, in the layered biological system, there is an initial temperature distribution $v_i(x)$ when the electromagnetic heating and/or the surface cooling begin.

According to the present approach, $v_i(x)$ can be chosen arbitrarily; nevertheless, it may be suitable, without loss of generality, to describe $v_i(x)$ as the steady-state solution in the case without electromagnetic heating and/or cooling.

In this paper, the transient temperature distribution in the layered biological system is obtained by applying the well-known method of finite differences [16], [17]. According to this method, the system's nonlinearity can be taken into account in the statement, both explicit and implicit, of the finite-difference equations. In the explicit statement, the Eulero form has been used, whereas in the implicit one, both the so-called "backward difference formula" and the Crank–Nicolson method [17] have been employed.

In the first case in each layer, the temperature is calculated point-by-point within the validity constraint $\Delta t/(\Delta x)^2 \leqslant c_n g_n / 2k_n$. In the second case, instead, because the value of Q^{tr} is required just at the time step in which the temperature is unknown, it is necessary to perform a projection; at each time step, the temperature distribution (i.e., the temperature at the chosen points) is obtained by solving a system of algebraic equations that, fortunately, is in an easy tridiagonal form [17]. In this case, the choice of the time step Δt is independent of the space step Δx, so that a reduction in computation time can be obtained. Nevertheless, a limitation to the value of Δt must be taken into account, depending on the projection that has been chosen.

In both cases, it may be suitable, even if not necessary, to perform a segment-linearization of the Q_n^{tr} functions, thus pointing out various threshold temperatures that diversify the thermoregulatory behavior of each layer into linear ranges. In general, however, the numerical program we have developed allows us to represent Q_n^{tr} in an arbitrary analytical form or by a set of input samples (experimental measurements, simulations, graphs, etc.) that are transformed into both a step function series and a reconstructed analytical form.

Moreover, the application of the finite-difference method allows us to take into account, in a simple way, slow time-dependent variations both in the mean power density of the incident field and in the coolant temperature; changes in such quantities can, in fact, be obtained at any time step.

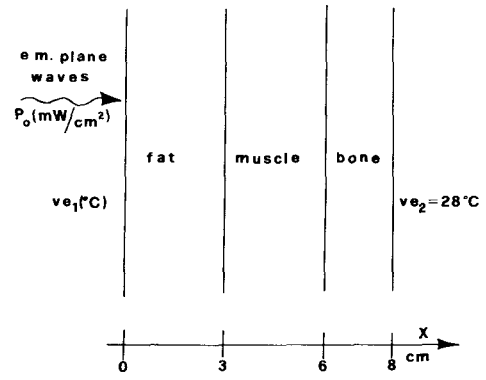

Fig. 1. Three-layered biological model.

III. Numerical Examples and Discussion

A first example of application is represented by the case of a three-layered biological model consisting of fat, muscle, and bone, as shown in Fig. 1.

Uniform plane waves at a mean power density P_0(mW/cm^2) impinge on the plane $x = 0$ in the normal direction, at a frequency of 2450 MHz. At this frequency, we have chosen the following values of the dielectric constant ϵ and electric conductivity σ for the various tissues [2]:

$$\begin{aligned} &\epsilon_m = 47\epsilon_0, && \epsilon_f = \epsilon_b = 5.5\epsilon_0 \\ &\sigma_m = 2.21 \text{ mho/m}, && \sigma_f = \sigma_b = .155 \text{ mho/m} \end{aligned} \tag{13}$$

where the subscripts m, f, b stand for muscle, fat, and bone, respectively, and ϵ_0 is the dielectric constant of free space.

Moreover, we have assumed that the temperature of the environment surrounding the layered model is $ve = 28$ °C, and that the surface $x = 0$ is cooled when the electromagnetic field is applied. Then, we have

$$\begin{aligned} &ve_1 = ve_2 = 28\ ^\circ C, && t < 0 \\ &ve_2 = 28\ ^\circ C, ve_1 \leqslant ve_2, && t \geqslant 0. \end{aligned} \tag{14}$$

In accordance with other papers (see, for example, [2], [4], [10]), we have chosen the following values of the thermal and physical parameters, which have been assumed to be constant:

$$\begin{aligned} &c_m g_m = 0.8025 \text{ cal/cm}^3\ ^\circ\text{C}, && k_m = 0.0012 \text{ cal/cm s} \\ &c_f g_f = 0.6025 \text{ cal/cm}^3\ ^\circ\text{C}, && k_f = 0.00055 \text{ cal/cm s} \\ &c_b g_b = 0.8568 \text{ cal/cm}^3\ ^\circ\text{C}, && k_b = 0.0035 \text{ cal/cm s} \end{aligned} \tag{15}$$

and

$$\beta_s|_{x=0} = \beta_s|_{x=1} = 0.25 \text{ cm}^{-1}. \tag{16}$$

In relation (16), for simplicity, the coefficients of the heat exchange with the external medium through the planes $x = 0$ and $x = 1$ have been assumed to be equal. However, the present problem statement and the numerical program we have developed allow us to consider different values of such coefficients, depending on the nature of the contact media and on their relative velocity [8].

Finally, the assumed nonlinear thermoregulatory behavior of the various tissues is presented in Figs. 2 and 3; as can be seen from these figures, some different examples of nonlinear functions for the muscle layer have also been considered.

Fig. 4 shows the transient temperature distribution in the case of curve b in Fig. 2, and for some values of the mean power density of the incident field ($P_0 = 100$ mW/cm^2 and $P_0 = 80$ mW/cm^2) and of the coolant temperature ($ve_1 = 17$ °C and $ve_1 = 10$ °C).

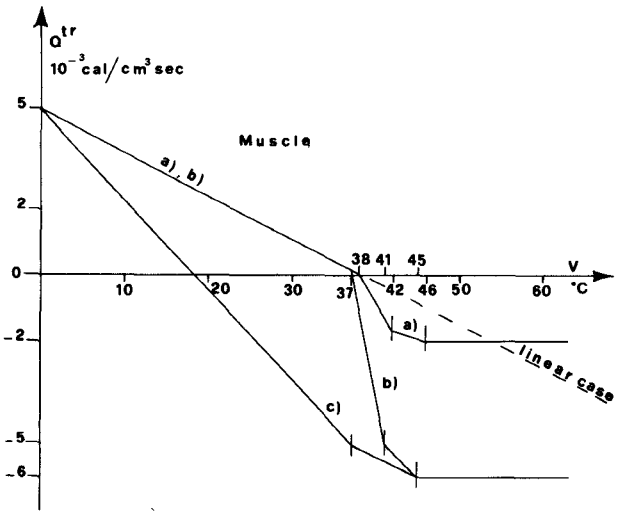

Fig. 2. Nonlinear thermoregultory function Q^{tr} of the muscle layer versus local temperature in the tissue.

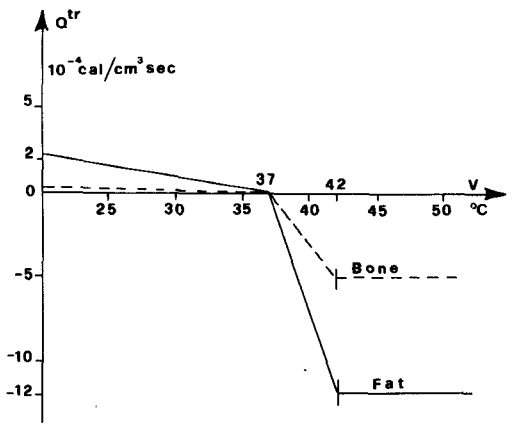

Fig. 3. Nonlinear thermoregulatory functions Q^{tr} of the bone (dashed line) and fat (continuous line) layers versus local temperatures in these tissues.

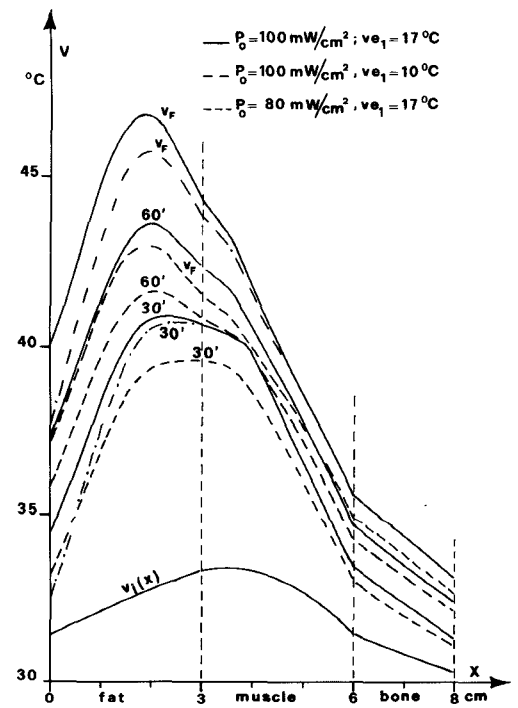

Fig. 4. Transient temperature distribution $v(x,t)$ in the three-layered biological model for the case of curve b in Fig. 2.

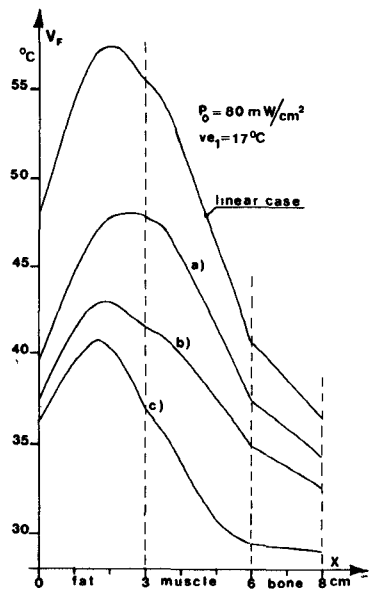

Fig. 5. Final temperature distributions v_F in the three-layered biological model for the various Q^{tr} functions of the muscle layer as shown in Fig. 2.

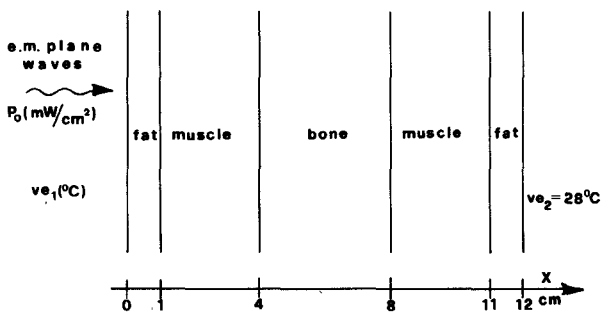

Fig. 6. Five-layered biological model.

The initial distribution $v_i(x)$ has been calculated via the same numerical program, but with $P_0 = 0$ and $ve_1 = 28°$ C (i.e., without electromagnetic heating and surface cooling).

In this figure, the curves labelled 30′ and 60′ represent the temperature distributions after 30 and 60 min of electromagnetic heating, respectively, while the curves labelled v_F represent the final distributions, i.e., those which differ in norm from the distribution of the previous time step by an arbitrary small reference quantity.

Fig. 5 illustrates the dependence of the final distribution on the thermoregulatory behavior of the muscle layer; this figure, in fact, shows the v_F curves obtained from the various Q^{tr} functions presented in Fig. 2, with $P_0 = 80$ mW/cm² and $ve_1 = 17$ °C.

Another example of appliction is represented by the perhaps more realistic case of a five-layered biological model, as shown in Fig. 6.

The transient temperature distribution given in Fig. 7 has been obtained under the same conditions as in the previous case, and the final configurations corresponding to the various thermoregulatory behaviors of the muscle layers are presented in Fig. 8.

The analysis of the above examples points out that the type of nonlinearity assumed causes the nonlinear thermoregulatory properties to lower the temperature distributions (see Figs. 5 and 8). Moreover, the smoother thermoregultory behavior of fat raises the temperature in the fat layer, while the slight rise in the temperature of the bone layer is due to the low electromagnetic absorption in this tissue.

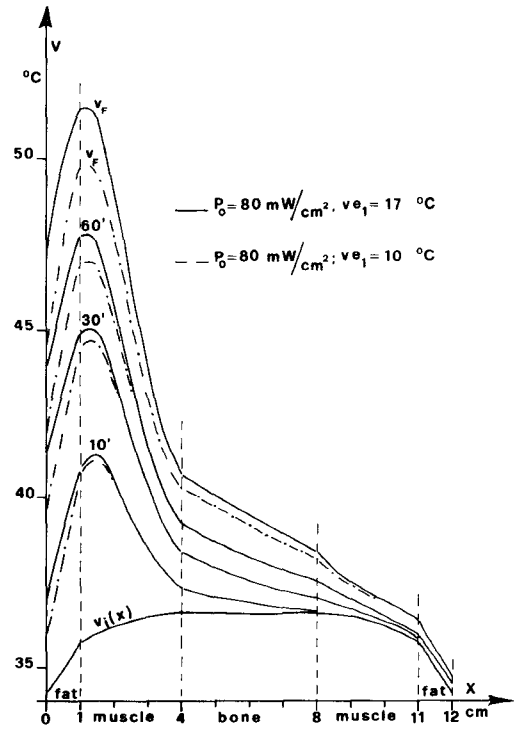

Fig. 7. Transient temperature distribution $v(x, t)$ in the five-layered biological model for the case of curve b in Fig. 2.

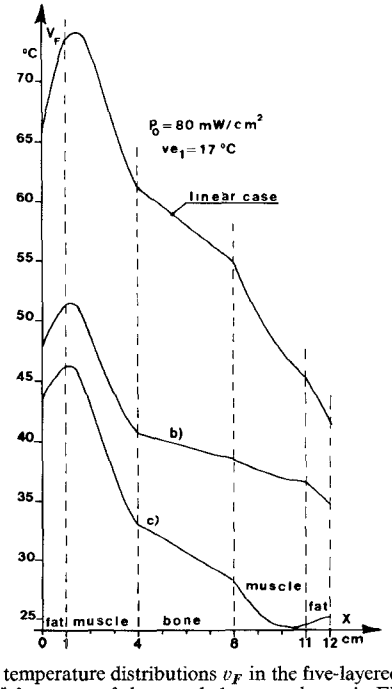

Fig. 8. Final temperature distributions v_F in the five-layered biological model for some Q^{tr} functions of the muscle layer as shown in Fig. 2 (linear b and c, respectively).

Figs. 4 and 7 also illustrate the different effects of the mean power density of the incident field, and of the coolant temperature.

A decrease in the coolant temperature produces a decrease in the temperature of the external surface, but not in the deep layers (for example, in the bone layer in Fig. 4). On the contrary, a variation in the temperature of the whole layered biological model is produced by a variation in the mean power density of the incident field, clearly as a function of the microwave power penetration and of the nonlinear thermal properties.

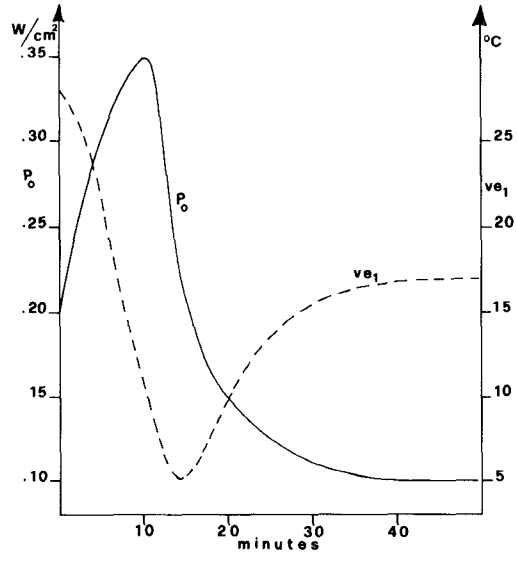

Fig. 9. Time variations in the mean power density P_0(mW/cm) of the incident field and in the coolant temperature ve_1 (°C).

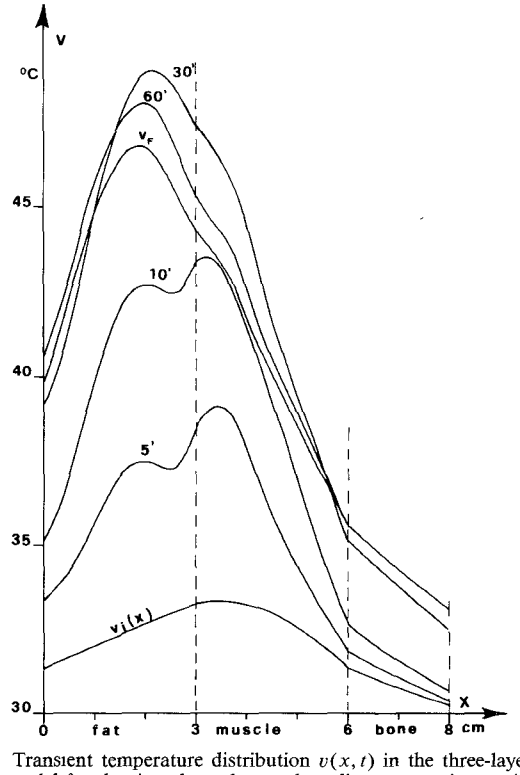

Fig. 10. Transient temperature distribution $v(x, t)$ in the three-layered biological model for the time-dependent and nonlinear case; time variations in P_0 and ve_1 are given in Fig. 9, while the nonlinear thermoregulatory behavior Q^{tr} of the muscle layer is given by curve b in Fig. 2.

Finally, an example of a time-dependent and nonlinear case is given by the three-layered biological model previously used (Fig. 1). Its dielectric and thermal properties have been chosen as in (13), (15), and (16), while curve b in Fig. 2 has been used as a nonlinear thermoregulatory function for the muscle layer.

Under the assumption of variations in the mean power density P_0 of the incident field and in the coolant temperature ve_1, as given in Fig. 9, we obtain the temporal evolution of the temperature distribution in the three-layered model, as shown in Fig. 10.

As can be seen from this figure, there is a fast initial increase in the temperature, corresponding to the initial increase in P_0 but balanced by the decrease in the coolant temperature. Subse-

quently, the temperature reaches its maximum value, and then the temperature distribution converges to its final configuration v_F.

REFERENCES

[1] J. G. Short and P. F. Turner, "Physical hyperthermia and cancer therapy," *Proc. IEEE*, vol. 68, pp. 133–142, Jan. 1980.

[2] A. W. Guy, J. F. Lehamann, and J. B. Stonebridge, "Therapeutic applications of electromagnetic power," *Proc. IEEE*, vol. 62, pp. 55–75, Jan. 1974.

[3] H. S. Carslaw and J. C. Jaeger, *Conduction of Heat in Solids*. Oxford: University Press, 1959.

[4] K. R. Foster, H. N. Kriticos, and H. P. Schwan, "Effect of surface cooling and blood flow on the microwave heating of tissues," *IEEE Trans. Biomed. Eng.*, vol. BME-25, pp. 313–316, Mar. 1978.

[5] R. Paglione, F. Sterzer, J. Mendecki, E. Friedhenthal, and C. Botstein, "27 MHz ridged waveguide applicators for localized hyperthermia treatment of deep-seated malignant tumors," *Microwave J.*, pp. 71–80, Feb. 1981.

[6] M. Gex-Fabry, J. Landry, M. Marceau, and S. Gagné, "Prediction of temperature profiles in tumors and surrounding normal tissues during magnetic induction heating," *IEEE Trans. Biomed. Eng.*, vol. BME-30, pp. 271–277, May 1983.

[7] F. Bardati, "Time-dependent microwave heating and surface cooling of simulating living tissues," *IEEE Trans. Microwave Theory Tech.*, vol. MTT-29, pp. 825–828, Aug. 1981.

[8] K. R. Foster, P. S. Ayyaswamy, T. Sundaraayan, and K. Ramakrishma, "Heat transfer in surface cooled objects subject to microwave heating," *IEEE Trans. Microwave Theory Tech.*, vol. MTT-30, pp. 1158–1166, Aug. 1982.

[9] R. J. Spiegel, D. M. Deffenbaugh, and J. E. Mann, "A thermal model of the human body exposed to an electromagnetic field," *Biolectromagn.*, vol. 1, pp. 253–270, 1980.

[10] J. L. Guerkin-Kern, L. Palas, M. Samsel, and M. Gautherie, "Hyperthermie micro-ondes: Influence du flux sanguin et des phénomènes thermorégulateurs," *Bull. Cancer* (Paris), vol. 68, pp. 273–280, Mar. 1981.

[11] S. Caorsi and A. Gialdini, "Riscaldamento elettromagnetico di modelli a strati piani di tessuti biologici: In-fluenza dei fenomeni termoregolatori," in *Proc. IV Nat. Conf. Elettromagnetismo Applicato*, Florence (Italy), Oct. 4–6, 1982, pp. 105–107.

[12] S. Caorsi, "Microwave heating of biological plane layers and nonlinear thermoregulatory effects," presented at the V Annual Meeting of The Bioelectromagnetics Society, Boulder, Co., June 12–16, 1983, p. GJ–58.

[13] S. Caorsi, "Electromagnetic heating and nonlinear thermoregulatory response of biological systems," in *Proc. 1983 URSI Int. Symp. on Electromagnetic Theory*, Santiago de Compostela (Spain), August 23–26, 1983, pp. 673–676.

[14] E. H. Grant, R. J. Sheppard, and G. P. South, *Dielectric Behaviour of Molecules in Solution*. Oxford: Clarendon Press, 1978.

[15] J. B. Hasted, *Aqueous Dielectrics*. London: Chapman and Hall, 1973.

[16] A. Wexler, "Computation of electromagnetic fields," *IEEE Trans. Microwave Theory Tech.*, vol. MTT-47, pp. 416–439, Aug. 1969.

[17] D. U. Von Rosemberg, *Methods for the Numerical Solution of Partial Differential Equations*. New York: American Elsevier, 1969.

Numerical Study of the Current Distribution on a Post in a Rectangular Waveguide

YEHUDA LEVIATAN, MEMBER, IEEE, DER-HUA SHAU, AND ARLON T. ADAMS, SENIOR MEMBER, IEEE

***Abstract*—A recently developed, rapidly converging moment solution for electromagnetic scattering by a single inductive post in a rectangular waveguide is extended to include the current induced on the post surface. The results are represented by a Fourier series and the first few terms are compared with available data. The excellent agreement demonstrates that this approach can yield an accurate solution. This rather simple procedure is even more attractive when other waveguide obstacles such as thick irises and posts of arbitrary shape, which require, in general, more than just a few Fourier terms for their current representation, are encountered.**

Manuscript received December 8, 1983; revised May 21, 1984. This work was partially supported by the Technion VPR fund "Philipson Fund for Research in Electrical Engineering."

Y. Leviatan is with the Department of Electrical Engineering, Technion-Israel Institute of Technology, Haifa, Israel.

D. Shau and A. T. Adams are with the Department of Electrical and Computer Engineering, Syracuse University, Syracuse, NY 13210.

I. INTRODUCTION

In a recent paper [1], Leviatan *et al.* have formulated the problem of a single inductive post in a rectangular waveguide in terms of an equivalent current, represented by a set of unknown current filaments placed either on or inside the post surface. Further, they applied a multiple point matching of the boundary condition on the post surface and solved for the unknown filamentary currents via the method of moments. These currents have then been employed to derive the scattering matrix and the equivalent T-network parameters for the post junction. The computed results showed good agreement with Marcuvitz's data [2] as far as this data goes, and demonstrated the feasibility of using this rather simple moment approach in solving the single-post as well as a variety of microwave discontinuities.

Although this paper [1] addresses many aspects of the single-post problem, its scope has been confined to the calculation of the equivalent T-network for the post two-port junction. Little attention has been paid to the current induced on the post surface. Knowledge of the surface induced current is not solely of academic interest, but of practical importance as well. For example, this current can be used in a perturbational solution to approximate the power dissipated in an imperfectly conducting post surface.

The main objective of this paper is to show that the simple multifilamentary representation for the equivalent current can accurately predict the actually induced current. The circular post is an attractive case study because pertaining results can be readily checked against results available, although not explicitly, in [3], where the first few terms of the Fourier series representation for the current have been employed in a Galerkin procedure. A successful use of the multifilamentary representation in calculating the post current would then enable simple current calculations for other waveguide obstacles such as thick irises and posts of arbitrary shape that require, in general, more than just a few Fourier terms for their current representation.

II. FORMULATION OF THE PROBLEM

The physical configuration of the problem under study is shown in Fig. 1, together with the coordinate system used. Following the procedure suggested in [1], we replace the post by N y-directed current filaments I_i, $i=1,2,\cdots,N$ equally spaced on a circular surface S_s taken to be either the same as the post surface S_o or concentric and inside S_o as shown in Fig. 2. These filaments function as an approximate equivalent current and, as such, generate a field which is approximately the field scattered by the post itself on and external to S_o.

The surface current induced on the circular post can be readily derived from the incident and scattered magnetic fields $\boldsymbol{H}^{\text{inc}}$ and $\boldsymbol{H}^{\text{scat}}$, as follows

$$\boldsymbol{J}_s = \hat{\boldsymbol{n}} \times (\boldsymbol{H}^{\text{inc}} + \boldsymbol{H}^{\text{scat}}) \tag{1}$$

where $\hat{\boldsymbol{n}}$ is a unit vector normal to the post surface. As shown in Fig. 1, $\hat{\boldsymbol{n}}$ is pointing towards the waveguide region. Using the coordinate system depicted in Fig. 1, $\hat{\boldsymbol{n}}$ is expressed as

$$\hat{\boldsymbol{n}} = -\boldsymbol{u}_x \cos\phi + \boldsymbol{u}_z \sin\phi. \tag{2}$$

0018-9480/84/1000-1411$01.00 ©1984 IEEE